Journal of The Electrochemical Society, **150** (3) C169-C174 (2003)
0013-4651/2003/150(3)/C169/6/$7.00 © The Electrochemical Society, Inc.

Preparation of Bi_2Te_3 Films by Electrodeposition from Solution Containing Bi-Ethylenediaminetetraacetic Acid Complex and TeO_2

Makoto Takahashi,[a,z] Yasuhiko Muramatsu,[a] Takao Suzuki,[a] Shoji Sato,[a] Makoto Watanabe,[a] Kouichi Wakita,[b] and Tetsuo Uchida[c]

[a]*Department of Applied Chemistry and* [b]*Department of Electronic Engineering, College of Engineering, Chubu University, Kasugai, Aichi 487-8501, Japan*
[c]*Department of Applied Chemistry, Nagoya Institute of Technology, Nagoya, Aichi 466-8555, Japan*

The electrodeposition of Bi-Te alloy films from nitric acid solutions containing TeO_2 and Bi-ethylenediaminetetraacetic acid (Bi-EDTA) complex was investigated. The product, composition, and surface morphology of Bi-Te alloy films were examined using an X-ray diffraction, inductively coupled plasma atomic emission spectroscopy, and scanning electron microscopy. In the solution containing TeO_2 and Bi-EDTA complex, bismuth deposits underpotentially in the potential range between −0.05 and −0.25 V, so that Bi_2Te_3 films are formed. In the potential region between −0.30 and −0.50 V, a limiting current is observed, the value of which is equal to the sum of the limiting currents observed for solutions containing TeO_2 or the Bi-EDTA complex. The composition of films deposited in this potential range can be controlled by the composition of the solution.
 [DOI: 10.1149/1.1542898]

Manuscript submitted March 15, 2002; revised manuscript received August 27, 2002. Available electronically February 6, 2003.

High-efficiency thin-film thermoelectric devices are interesting for applications in the microelectronics industry, such as thermoelectric coolers[1] and thermoelectric generators.[2] Bismuth telluride (Bi_2Te_3) and its solid solutions are well known as good thermoelectric materials for near-room-temperature applications. Bismuth telluride and its solid solution films have been prepared using a number of techniques, such as sputtering,[3-5] metallorganic chemical vapor deposition (MOCVD),[6,7] molecular beam epitaxy (MBE),[8-10] and electrodeposition.[11-13] Electrodeposition may offer a low-cost growth method for high-quality metal, alloy, and semiconductor films.

We have reported the preparation of Bi_2Te_3 and its solid solution films by electrodeposition.[14,15] In these previous studies, we used the element Bi as the source of Bi^{3+} ions. However, since Bi^{3+} is easily converted into the hydrolysis product, $Bi(OH)_3$, a hydrous polymer, it is difficult to prepare the electrolytic bath solution and as a result, reproducibility is low. The compositions of films can be controlled only by the composition of the electrolytic bath solution and cannot be controlled by the electrodeposition potential. Therefore, we reasoned that if the hydrolysis of Bi^{3+} ions could be hindered by using the Bi-EDTA complex, it would be easier to prepare the electrolytic bath solution and reproducibility would be improved. In this paper, we report the relation between the deposition conditions and the composition of films.

Experimental

Bismuth telluride and its alloy films were electrodeposited from aqueous solutions containing various concentrations of Bi-ethylenediaminetetraacetic acid (EDTA) complex and TeO_2, pH 1.0 ± 0.1, on Ti sheets. Ti sheets were degreased with chloroform and ethanol, treated with a 15% HF solution to remove any oxide layer, and washed with deionized water before use. Reagent-grade HNO_3, EDTA·2Na purity 99.5%, $Bi(NO_3)_3$ (purity 99.9%), and TeO_2 (purity 99%) were used without further purification. Water was purified using the Milli-Q water purification system (Millipore Corporation). The usual three-electrode cell was used for the electrodeposition of films and films were potentiostatically deposited using a potentiostat (Hokuto Denko, HA-151). A platinum wire and an Ag/AgCl electrode were used for counter and reference electrodes, respectively. The current-potential relations were measured with a potentiostat and *X-t* recorder. The deposition of films and the electrochemical measurements were conducted at room temperature in the dark, after the electrolytic bath solutions were deaerated by passing N_2 or Ar gas through the solution for about 15 min.

X-ray diffraction (XRD) patterns were obtained with a diffractometer (Philips Co., Ltd., RHL-P610CP) using Cu $K\alpha_1$ radiation. Scanning electron microscopy (SEM) analyses were carried out using a Hitachi S-3500 scanning electron microscope. The composition of films was determined by inductively coupled plasma atomic emission spectroscopy (ICP-AES) (Seiko Instruments SPS-7000). Film thickness was determined using a Surfcorder model SE-3F stylus-type surface roughness measuring instrument (Kosaka Laboratory, Ltd.).

Results

Electrochemical measurements.—Figure 1 shows the current-potential relations observed in various solutions: (a) 0.5 mM TeO_2 (○) and (b) 1.0 mM Bi-EDTA complex (△), at pH 1.0 ± 0.1 on Au substrates. During the measurements shown in Fig. 1a, the cathodic current began to flow at 0 V *vs.* Ag/AgCl, and at potentials more negative than −0.05 V the cathodic current increased rapidly. The gray films then grew. A limiting current was observed at potentials between −0.20 and −0.55 V. This cathodic current was due to the reduction of $HTeO_2^+$ to metallic Te (Eq. 1) and the limiting current was due to diffusion of the $HTeO_2^+$ ion. The cathodic current again increased rapidly at potentials more negative than −0.60 V, and many bubbles were formed on the electrode surface, suggesting the current increase was due to the evolution of H_2

$$HTeO_2^+ + 3H^+ + 4e^- \rightarrow Te + 2H_2O$$

$$E_0 = 0.329 \text{ V } \textit{vs.} \text{ Ag/Cl} \qquad [1]$$

For the measurements shown in Fig. 1b, the cathodic current began to flow at 0 V and a low limiting current was observed at potentials between −0.05 and −0.20 V. However, no change on the electrode surface was observed. The cathodic current increased rapidly at potentials more negative than −0.25 V and gray products were formed. A limiting current was observed at potentials between −0.40 and −0.50 V, which increased with increasing Bi-EDTA concentration. Therefore, this cathodic current was due to the reduction of Bi-EDTA complex to metallic Bi (Eq. 2) and the limiting current was due to the Bi-EDTA complex ion diffusion. At potentials below −0.60 V, the cathodic current H_2 evolution began again

[z] E-mail: thinfilm@isc.chubu.ac.jp

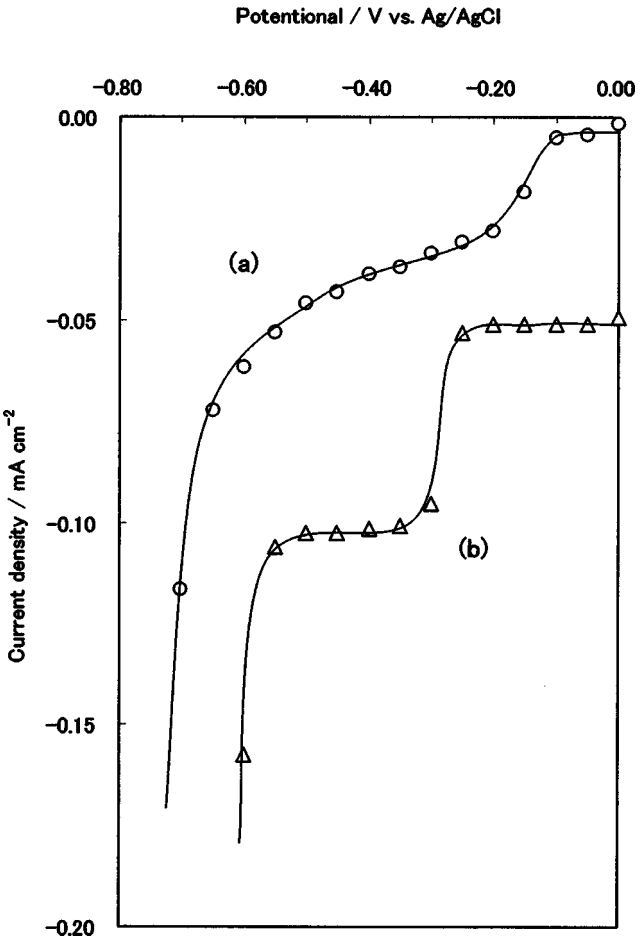

Figure 1. Current-potential relations observed on Au electrode in a nitric acid solution (pH1.0 ± 0.1) containing (a,○) 0.5 mM TeO_2 and (b,△) 1.0 mM Bi-EDTA complex.

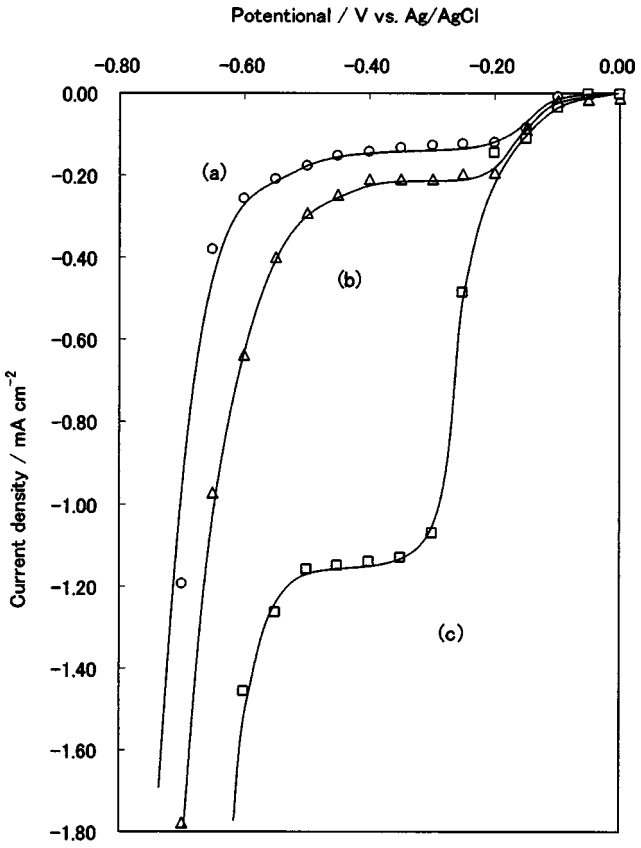

Figure 2. Current-potential relations observed on Au electrode in a nitric acid solution (pH1.0 ± 0.1) containing 0.5 mM TeO_2 and various concentrations of Bi-EDTA complex: (a,○) 1.0, (b,△) 2.0, and (c,□) 12.0 mM.

$$Bi\text{-}Y^- + 4H^+ + 3e^- \rightarrow Bi + H_4Y^- \qquad E_0 = -0.013 \text{ V } \textit{vs.} \text{ Ag/AgCl} \qquad [2]$$

(Y: EDTA (ethylenediamine tetraacetic acid))

where E_0 is a standard redox potential of Reaction 2 and Y is EDTA. Its value was calculated using the standard redox potential of Bi^{3+}/Bi and the stability constant for the Bi-EDTA complex formation.

Figure 2 displays the current-potential relations observed in solutions containing 0.5 mM TeO_2 and various concentrations of Bi-EDTA complex: (a) 1.0, (b) 2.0, and (c) 12.0 mM. In Fig. 2a, at potentials more negative than −0.05 V the cathodic current increased rapidly and black films were deposited on the electrode surface. The limiting current was observed at potentials between −0.20 and −0.30 V, and was larger than those observed in Fig. 1a and b. The cathodic current gradually increased as the electrode potential decreased. The increase of cathodic current due to the evolution of H_2 was again observed at potentials more negative than −0.50 V. In Fig. 2b and c, at potentials more negative than −0.05 V the cathodic current increased and black films were deposited. In the potential range between −0.10 and −0.20 V, the same shoulder is observed. The cathodic currents rapidly increase again and the limiting current is observed in the potential range between −0.35 and −0.45 V. These observed values are equal to the sum of the limiting current for the solution containing TeO_2 and the limiting current observed in the solution containing the Bi-EDTA complex. At potentials below −0.50 V, the cathodic current due to the evolution of H_2 began to increase, again.

The dependence of the limiting current observed at −0.20 V on the Bi-EDTA complex concentration for the solutions in which TeO_2 concentrations were kept constant at (○) 0, (△) 0.5, and (□) 1.0 mM are shown in Fig. 3. In the solution not containing TeO_2, the cathodic current is not dependent on the Bi-EDTA complex concentration. However, when the solution contained TeO_2, the cathodic currents at −0.20 V increased linearly with the increase in the Bi-EDTA complex concentration, and above a critical concentration of the Bi-EDTA complex the cathodic currents showed constant values. The slopes in the linear parts are about 0.08 and are equal to each other. The values of the intercepts for the plots agreed with the currents observed at −0.20 V in the solution containing only TeO_2. These results imply that at −0.20 V, when elemental Te exists on the electrode surface, Bi can codeposit underpotentially onto the electrode. The dependence of the limiting current observed at −0.45 V on the Bi-EDTA complex concentration, for the solutions in which TeO_2 concentrations were kept constant at (●) 0, (▲) 0.5, and (■) 1.0 mM, are shown in Fig. 3. For each case, the limiting current is proportional to the Bi-EDTA complex concentration. The slopes of these plots have the same value of about 0.09, similar to the value obtained in Fig. 3. This result implies that at potentials between −0.35 and −0.45 V, the limiting current for the diffusion of the Bi-EDTA complex is not affected by the reduction of $HTeO_2^+$ to metallic Te on the electrode surface. The values of the intercepts for the plots agreed with the limiting currents observed in the solution containing only TeO_2. The limiting current observed at potentials between −0.40 and −0.55 V, in the solutions containing Bi-EDTA

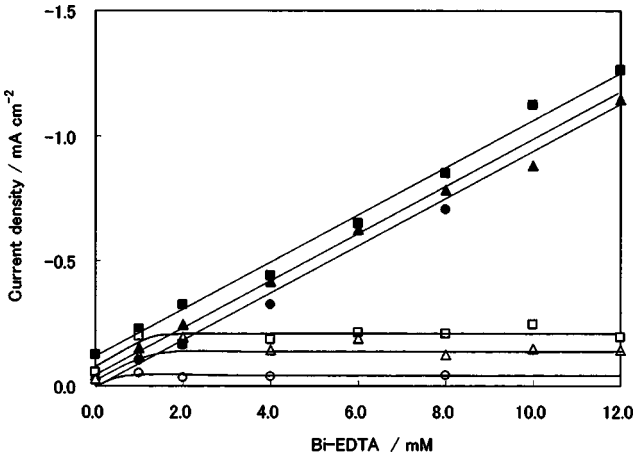

Figure 3. The dependence of the cathodic current at −0.20 V *vs.* Ag/AgCl on Bi-EDTA complex concentration for the nitric acid solutions in which TeO_2 concentrations are: (○) 0, (△) 0.5, and (□) 1.0 mM. The dependence of the limiting current at −0.45 V on Bi-EDTA complex concentration for the nitric acid solutions in which TeO_2 concentrations are: (●) 0, (▲) 0.5, and (■) 1.0 mM.

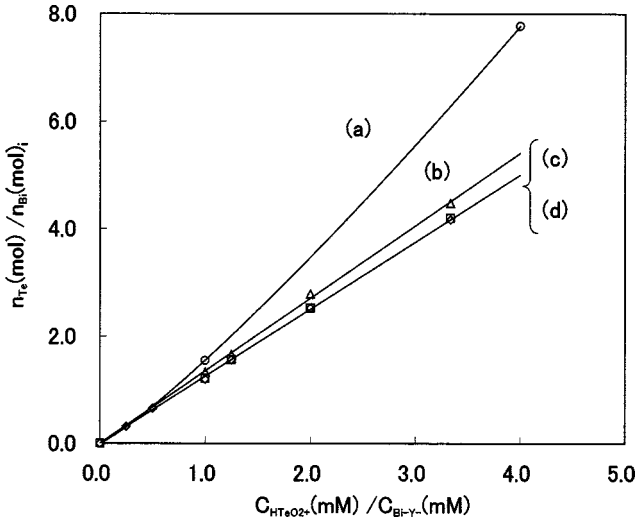

Figure 5. The relations between the ratio of TeO_2 concentration to Bi-EDTA complex concentration ($C_{HTeO_2^+}/C_{Bi\text{-}EDTA}$) and the composition ($n_{Te}/n_{Bi}$) of films deposited at various deposition potentials: (a,○) −0.125, (b,△) −0.150, (c,□) −0.30, and (d,◇) −0.45 V.

complex and TeO_2, is the sum of the limiting currents observed for TeO_2 and Bi-EDTA complex, respectively.

Electrodeposited film compositions.—The relations between the deposition potential and the composition (mole ratio of Te to Bi) of films deposited in solutions containing 1.0 mM TeO_2 and various Bi-EDTA complexes are shown in Fig. 4. In the films deposited in the solution containing 0.5 mM Bi-EDTA complex (Fig. 4a), the mole ratio (Te/Bi) decreases up to −0.30 V as the deposition potential becomes negative and reaches a constant value of 2.53 ± 0.02. In the solution containing 0.8 mM Bi-EDTA complex (Fig. 4b), the mole ratio (Te/Bi) decreases up to −0.20 V as the deposition potential becomes negative, and reaches a constant value of 1.59 ± 0.03. In the solution containing 1.0 mM Bi-EDTA complex (Fig. 4c), the mole ratio (Te/Bi) decreases up to −0.175 V as the deposition potential becomes negative and reaches a constant value of 1.20 ± 0.02. The potential where the mole ratio (Te/Bi) is a constant value moved toward positive potentials with an increase in the Bi-EDTA complex concentration. The observed constant value

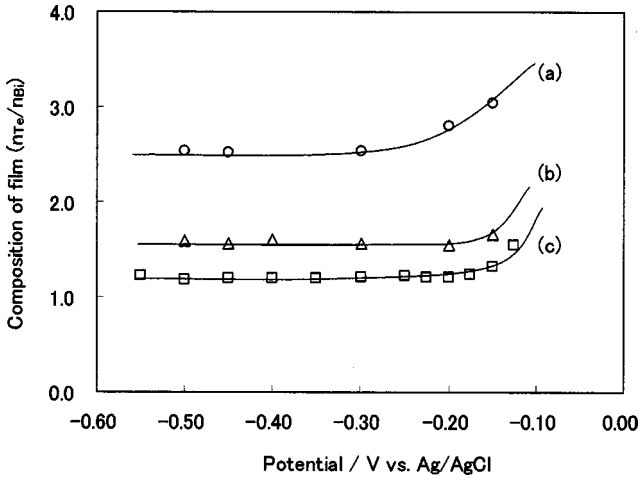

Figure 4. The relations between the composition (mole ratio of Te to Bi) of films deposited in solutions containing 1.0 mM TeO_2 and various Bi-EDTA complex concentration: (a,○) 0.5, (b,△) 0.8, and (c,□) 1.0 mM, and the deposition potential.

decreased with the increase in the Bi-EDTA complex concentration. The relation between the ratio of TeO_2 concentration and Bi-EDTA complex concentration ($C_{TeO_2}/C_{Bi\text{-}EDTA}$) and the composition ($n_{Te}/n_{Bi}$) of films deposited at various deposition potentials are shown in Fig. 5. For the films deposited at −0.125 V (Fig. 5a), the mole ratio (Te/Bi) in the film increased rapidly but not linearly with an increase in the ratio of TeO_2 concentration to Bi-EDTA complex concentration. For the films deposited at potentials more negative than −0.15 V, the mole ratio (n_{Te}/n_{Bi}) in the films increased linearly with an increase in the ratio of TeO_2 concentration to Bi-EDTA complex. For films deposited between −0.35 and −0.45 V, the relations between the ratio of the TeO_2 concentration to the Bi-EDTA complex concentration ($C_{TeO_2}/C_{Bi\text{-}EDTA}$) and the composition ($n_{Te}/n_{Bi}$) of films fall on the same line. The purpose of our investigation is the preparation of Bi-rich p-Bi_2Te_3 and Te-rich n-Bi_2Te_3 from the same solution by controlling the deposition potential. From the results in Fig. 5, therefore, the experimental condition that seems to satisfy our purpose is a concentration ratio of the solution of 1.16. In this solution containing 1.0 mM TeO_2 and 0.86 mM Bi-EDTA, Te-rich n-Bi_2Te_3 films are deposited at potentials more positive than −0.25 V, and Bi-rich p-Bi_2Te_3 films are deposited at potentials more negative than −0.25 V.

X-ray diffraction patterns of electrodeposited films.—The XRD patterns of films deposited at various potentials in the solution containing 1.0 mM TeO_2 and 0.86 mM Bi-EDTA complex are shown in Fig. 6. In the diffraction pattern of the film deposited at −0.125 V (Fig. 6a), eleven broad diffraction peaks are observed at 2θ = 8.6, 17.6, 23.8, 27.8, 38.0, 40.2, 41.2, 45.1, 50.5, 53.1, and 57.3. The peaks observed at 2θ = 8.6, 17.6, 23.8, 27.8, 38.0, 40.2, 41.2, 50.5, and 57.3 correspond to Bi_2Te_3[16] or several Bi-Te alloy compounds (*i.e.*, BiTe,[17] Bi_4Te_3,[18] etc.). Since the spacing of crystal faces of Bi-Te alloy compounds are similar to each other, products are not exactly determined by the XRD patterns. The shoulder of diffraction peaks observed at 2θ = 23.8, 27.8, 38.0, 40.2, 50.5, and 57.3 corresponded to the (100), (101), (102), (110), (201), and (202) planes of Te metal,[19] respectively. This result indicates that this film is composed of a mixture of several Bi-Te compounds and Te metal. When the film was deposited at −0.25 V (in Fig. 6b), the diffraction peaks observed at 2θ = 17.6, 23.4, 27.7, 38.4, 40.8, 50.2, and 57.4 corresponded to peaks for Bi_2Te_3 or Bi-Te alloy compounds. The

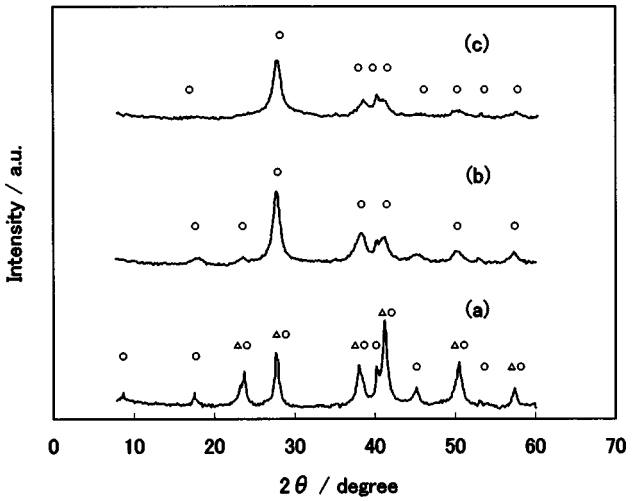

Figure 6. The XRD patterns of film deposited at various potentials in the solution containing 1.00 mM TeO_2 and 0.86 mM Bi-EDTA complex: (a) −0.125, (b) −0.250, and (c) −0.450 V; (○) Bi-Te alloy and (△) Te.

shoulder of diffraction peaks observed at $2\theta = 27.7$, 38.4, 40.2, and 50.2, and the diffraction peaks at $2\theta = 45.4$ corresponded to the (101), (102), (110), (201), and (003) planes of Te metal, respectively. In the diffraction pattern of the film deposited at −0.45 V (Fig. 6c), many diffraction peaks are observed. The diffraction peaks at $2\theta = 17.8$, 27.8, 37.6, 40.2, 41.1, 45.0, 50.2, 53.1, and 57.5 are due to Bi_2Te_3 or Bi-Te alloy compounds. When these films were annealed at 350°C for 60 min in N_2, the intensity of diffraction peaks due to Bi_2Te_3 increased and a new diffraction peak was observed at $2\theta = 8.8$. This new diffraction peak corresponds to the (003) plane of Bi_2Te_3, which characterizes Bi_2Te_3 lamellar compound.[16] Therefore, the as-grown films deposited in the solution containing 1.0 mM TeO_2 and 0.86 mM Bi-EDTA complex, at potentials more negative than −0.20 V, consist of Bi_2Te_3. These results indicate that the film composition is not only controlled by the composition of the solution, but also by the deposition potential.

Surface morphology of films.—Figure 7 shows SEM micrographs of films deposited from solution containing 1.0 mM TeO_2 and 0.86 mM Bi-EDTA complex at various deposition potentials, (a) −0.20, (b) −0.25, (c) −0.30, and (d) −0.45 V. The average film thickness used for the SEM observations was 1.7 ± 0.3 μm. For the film deposited at −0.20 V (in Fig. 7a), the film consisted of small chestnut-like particles and the surface of the film was smooth. For the film deposited at −0.25 V (in Fig. 7b), the film consisted of rounded particles that resembled balls of yarn. The particle size was 4-6 μm. For the films deposited at −0.30 V (in Fig. 7c), the film consisted of two types of particles. One type was rounded particles smaller than 3 μm. The other type was layered structures of leafy particles (dendrite). From the results of energy-dispersive X-ray (EDX) measurements, though the shapes of the particles were different, no difference in their compositions was detected. For the films deposited at potentials more negative than −0.45 V (in Fig. 7d), the film consisted of dendrite particles. From these results, the effect of the film composition on the film morphology can be summarized as follows. When the film is deposited at potentials more positive than −0.28 V, the film composition (n_{Te}/n_{Bi}) is larger than 0.50, and the film is composed of rounded particles and has a relatively smooth surface. When the film is deposited at potentials more negative than −0.28 V, the composition (n_{Te}/n_{Bi}) is slightly lower than 1.50, and the film consists of two types of particles [the rounded particles and the layered, leafy particles (dendrite)].

Discussion

The results are summarized as follows:

1. Use of Bi-EDTA complex facilitates preparation of the electrolytic bath, because the Bi-EDTA complex suppresses the hydrolysis reaction of aqueous Bi^{3+} ions.
2. When Te exists on the electrode, Bi deposits underpotentially in the potential range between −0.05 and −0.25 V.
3. The cathodic currents observed in the potential range between −0.05 and −0.20 V in the solution containing TeO_2 are due to the underpotential deposition of Bi-EDTA, and those values increase with an increasing Bi-EDTA complex concentration. The maximum values of these currents due to the underpotential deposition depend on the TeO_2 concentration.
4. In the potential range between −0.05 and −0.30 V, the film composition can be controlled by the deposition potential and the composition of the electrolytic bath.
5. The films electrodeposited in the potential range between −0.05 and −0.55 V are mixtures of Te metal and Bi-Te alloy compounds (*e.g.*, Bi_2Te_3, BiTe, $Bi_{2+x}Te_{3-x}$, $Bi_{14}Te_6$, etc.).
6. The Bi concentration in the films increases with an increase in Bi-EDTA complex concentration in the solution.
7. The limiting current observed in the potential region between −0.30 and −0.50 V is equal to the sum of the limiting currents observed for the TeO_2 and Bi-EDTA complex solutions.

In the following, we discuss the formation reaction of Bi-Te alloy films. First, we divide the potential range into two potential ranges, Range I and Range II. Range I is the potential region between −0.05 and near −0.25 V, and in this region the underpotential deposition of Bi-EDTA complex to Bi-Te alloy can be observed. Range II is the potential region between −0.30 and −0.50 V. In this range, Bi-EDTA complex can be reduced to Bi metal and both limiting currents due to $HTeO_2^+$ ion and Bi-EDTA complex are observed.

In Range I, the following electrode reactions are involved in the formation of Bi-Te alloys

$$HTeO_2^+ + 3H^+ + 4e^- \rightarrow Te(s) + 2H_2O \quad [1]$$

$$a\text{Bi-Y}^- + b\text{Te}(s) + 4aH^+ + 3ae^- \rightarrow \text{Bi}_a\text{Te}_b + aH_4Y^- \quad [3]$$

$$(a = 1,2,3,...b = 1,2,3...)$$

where Bi_aTe_b is an intermetallic compound (*i.e.*, BiTe, Bi_2Te_3, $Bi_{14}Te_6$, etc.). From these results (Fig. 3, 4, 5, and 6), it is assumed that the rate of Reaction 3 is several times faster than that of Reaction 1. The Bi-EDTA complex is reduced to Bi-Te alloy compounds as soon as $HTeO_2^+$ ion is reduced to metallic Te. If the amount of Te element supplied to the electrode is limited, the current due to the reduction of the Bi-EDTA complex increases with the increase in the Bi-EDTA complex concentration up to a critical concentration limited by the maximum rate of Reaction 3. Therefore, the results in Fig. 3a and b are explained as follows. Until the amount of Bi supplied to the electrode agrees with the maximum amount of Bi consumed by Reaction 3, the cathodic current depends on the Bi-EDTA complex concentration. After that, the cathodic current does not depend on the Bi-EDTA concentration and maintains a constant value.

In the Range II, the following electrode reactions are involved in the formation of Bi-Te alloys

$$HTeO_2^+ + 3H^+ + 4e^- \rightarrow Te(s) + 2H_2O \quad [1]$$

$$\text{Bi-Y}^- + 4H^+ + 3e^- \rightarrow \text{Bi}(s) + H_4Y^- \quad [2]$$

$$a\text{Bi}(s) + b\text{Te}(s) \rightarrow \text{Bi}_a\text{Te}_b(s) \quad [4]$$

$$(a = 1,2,3,...b = 1,2,3...)$$

where Bi_aTe_b is an intermetallic compound (*i.e.*, BiTe, Bi_2Te_3, $Bi_{14}Te_6$, etc.). In this potential range, Reactions 2 and 4, which are the solid-state reactions of Bi-Te alloy compounds, are introduced.

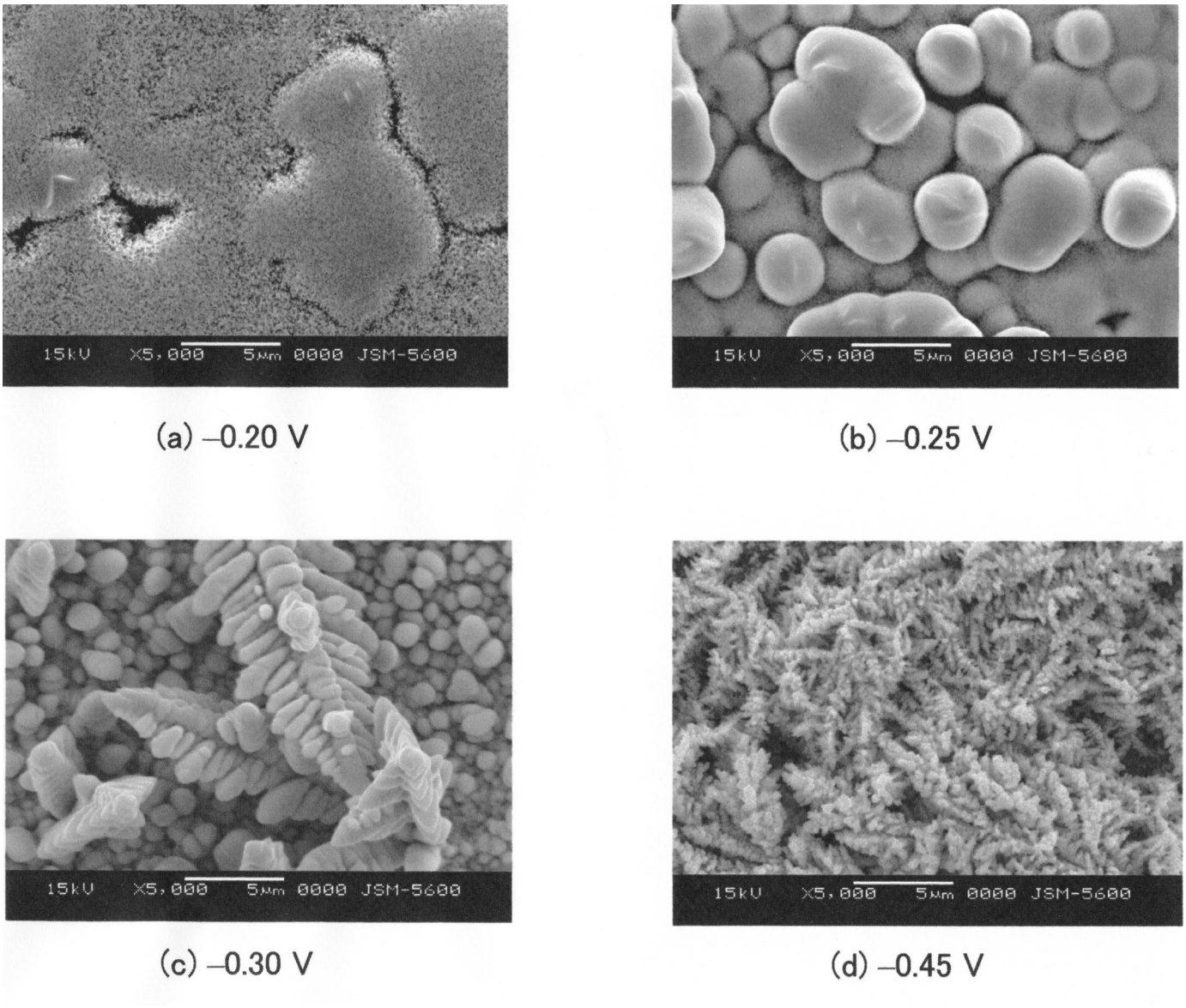

Figure 7. The SEM micrographs of films deposited in the solution containing 1.00 mM TeO_2 and 0.86 mM Bi-EDTA complex at various deposition potentials: (a) −0.20, (b) −0.25, (c) −0.30, and (d) −0.45 V.

These reactions can be considered to be the transformation of Reaction 3. The observed limiting current is equal to the sum of limiting currents for Reactions 1 and 2. The limiting currents due to Reactions 1 and 2 are expressed by Eq. 5 and 6, respectively

$$i_{Te} = -(4^{\star}D_{HTeO_2^+}{}^{\star}F^{\star}C_{HTeO_2^+})/\delta_{HTeO_2^+}, \quad [5]$$

$$i_{Bi} = -(3^{\star}D_{Bi\text{-}Y^-}{}^{\star}F^{\star}C_{Bi\text{-}Y^-})/\delta_{Bi\text{-}Y^-} \quad [6]$$

where $D_{HTeO_2^+}$ ($D_{Bi\text{-}Y^-}$), $\delta_{HTeO_2^+}$($\delta_{Bi\text{-}Y^-}$), and $C_{HTeO_2^+}$($C_{Bi\text{-}Y^-}$) are the diffusion coefficient, the thickness of the diffusion layer, and the concentration of $HTeO_2^+$(Bi-Y^-), respectively. The limiting current observed at −0.45 V in solution containing $HTeO_2^+$ and Bi-Y^- is expressed by Eq. 7

$$i_{obs} = i_{Te} + i_{Bi} = -(4^{\star}D_{HTeO_2^+}{}^{\star}F^{\star}C_{HTeO_2^+})/\delta_{HTeO_2^+} - (3^{\star}D_{Bi\text{-}Y^-}{}^{\star}F^{\star}C_{Bi\text{-}Y^-})/\delta_{Bi\text{-}Y^-} \quad [7]$$

This equation is supported by the results in Fig. 3. Therefore, at deposition time, t (s), the mole ratio Te(mol)/Bi(mol) (n_{Te}/n_{Bi}) is given by Eq. 8

$$n_{Te}/n_{Bi} = (D_{HTeO_2^+}/\delta_{HTeO_2^+})/(D_{Bi\text{-}Y^-}/\delta_{Bi\text{-}Y^-})^{\star}(C_{HTeO_2^+}/C_{Bi\text{-}Y^-}) \quad [8]$$

where ($D_{HTeO_2^+}/\delta_{HTeO_2^+}$) and ($D_{Bi\text{-}Y^-}/\delta_{Bi\text{-}Y^-}$) are given by the slopes of the relation between the limiting current and TeO_2 and Bi-Y complex concentrations, respectively. Using the obtained values, Eq. 8 is rewritten as Eq. 9

$$n_{Te}/n_{Bi} = 1.29^{\star}(C_{HTeO_2^+}/C_{Bi\text{-}Y^-}) \quad [9]$$

The relation between the mole ratio (n_{Te}/n_{Bi}) of the film and the ratio of molar concentration ($C_{HTeO_2^+}/C_{Bi\text{-}Y^-}$) in the solution is shown in Fig. 8. In this figure, ○ and □ represent the experimental values and the calculated values using Eq. 9. The calculated values agree with the experimental values over the wide range of Bi-EDTA

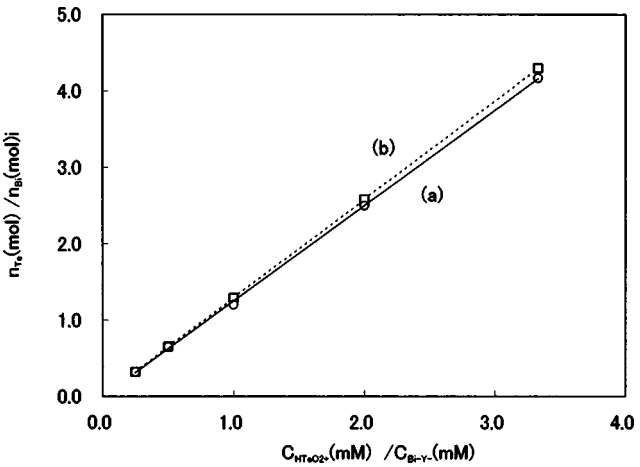

Figure 8. The relation between the mole ratio (n_{Te}/n_{Bi}), of the films and the ratio of molar concentration ($C_{HTeO_2^+}/C_{Bi\text{-}Y}$) in the solution: (a,○, ——) the experimental values and (b,□, — — —) calculated values.

concentration. In our previous studies, when the Bi^{3+} ion concentration increased, the hydrolysis of Bi^{3+} occurred, so that the calculated values (n_{Te}/n_{Bi}) departed from the experimental values. However, using the Bi-EDTA complex as the source of Bi element, the hydrolysis of bismuth ion is suppressed so that the composition of the film can be controlled over the wide range of Bi-EDTA concentration.

Conclusions

Bi-Te alloy films are electrodeposited from acidic solutions containing TeO_2 and Bi-EDTA complex. Using Bi-EDTA complex as a Bi source, the hydrolysis of Bi^{3+} ion is suppressed so that the films can be deposited over a wide range of Bi-EDTA concentration, and Bi-Te alloy films are underpotentially deposited in the potential range between −0.05 and −0.25 V. When films are deposited at the potential region between −0.30 and −0.50 V, the composition of the film can be expressed by Eq. 9.

Acknowledgment

This work was supported by a grant from the High-Tech Research Center Establishment Project of Ministry of Education, Science, Sports and Culture. This work was partially supported by Grants-in-Aid for Scientific Research on Priority Area of Electrochemistry of Ordered Interfaces (no. 09237101).

Chubu University assisted in meeting the publication costs of this article.

References

1. T. Ohta, T. Uesugi, T. Tokiai, M. Nosaka, and T. Kajikawa, *Trans. Inst. Electr. Eng. Jpn., Part B*, **111-B**, 670 (1991).
2. S. Hava, H. B. Sequeira, and R. G. Hunsperger, *J. Appl. Phys.*, **58**, 1727 (1985).
3. H. Noro, K. Sato, and H. Kagechika, *J. Appl. Phys.*, **73**, 1252 (1993).
4. Y. H. Shing, Y. Chang, A. Mirshafii, L. Hayashi, S. S. Roberts, J. Y. Josefowicz, and N. Tran, *J. Vac. Sci. Technol. A*, **1**, 503 (1983).
5. M. J. McCulley, G. W. Neudeck, and G. L. Liedl, *J. Vac. Sci. Technol.*, **10**, 391 (1973).
6. A. Giani, A. Boulouz, F. Pascal-Delannoy, A. Fourcaran, and A. Boyer, *Thin Solid Films*, **315**, 99 (1998).
7. R. Venkatasubramanian, T. Colpitts, E. Watko, M. Lamvik, and N. El-Masry, *J. Cryst. Growth*, **170**, 817 (1997).
8. S. Cho, Y. Kim, A. DiVenere, G. K. Wong, J. B. Ketterson, and J. R. Meyer, *Appl. Phys. Lett.*, **75**, 1401 (1999).
9. E. Charles, E. Groubert, and A. Boyer, *J. Mater. Sci. Lett.*, **7**, 575 (1998).
10. A. Boyer and E. Cisse, *Mater. Sci. Eng., B*, **B13**, 103 (1992).
11. A. L. Prieto, M. S. Sander, M. S. Martin-Gonzalez, R. Gronsky, T. Sands, and A. M. Stacy, *J. Am. Chem. Soc.*, **123**, 7160 (2001).
12. Y. Miyazaki and T. Kajitani, *J. Cryst. Growth*, **229**, 542 (2001).
13. P. Magri, C. Boulanger, and J. M. Lecuire, *J. Mater. Chem.*, **6**, 773 (1996).
14. M. Takahashi, Y. Oda, T. Ogino, and S. Furuta, *J. Electrochem. Soc.*, **140**, 2550 (1993).
15. M. Takahashi, Y. Katou, K. Nagata, and S. Fruta, *Thin Solid Films*, **240**, 7 (1994).
16. JCPDS Card No. 15-863.
17. JCPDS Card No. 31-200.
18. JCPDS Card No. 33-216.
19. JCPDS Card No. 27-871.